J. Phys. B: Atom. Molec. Phys., Vol. 12, No. 3, 1979. Printed in Great Britain

Excitation of $^1S(1s, 3s)$ state of helium by electron impact in the Glauber approximation

A C Roy† and N C Sil‡

†Department of Physics, University of Kalyani, Kalyani-741235, India
‡Department of Theoretical Physics, Indian Association for the Cultivation of Science, Calcutta-700 032, India

Received 1 June 1978

Abstract. We report Glauber cross sections for the electron-impact optically-forbidden transition $^1S(1s, 3s) \leftarrow {}^1S(1s)^2$ in helium in the incident energy range 29·2 to 500 eV. The Glauber amplitude is calculated using an alternative procedure for the evaluation of the modified Lommel function instead of the usual series representation which requires very high precision arithmetic for the intermediate values of the argument. The present results for both the differential and integral cross sections in the single-particle Glauber approximation (SPGA) and the full Glauber approximation (GA) are compared with experimental findings and with the predictions of recent theoretical calculations. We find that the GA predicts the shape of differential cross sections even at a few electron volts beyond threshold. At higher incident energies the GA yields cross sections in good agreement with experiment. At low energies the SPGA deviates strongly from the GA and fails to predict the angular distributions of scattered electrons.

1. Introduction

Since 1968 the Glauber approximation (GA) (Glauber 1959) has been applied extensively to atomic collisions (Gerjuoy and Thomas 1974, Byron and Joachain 1977). One of the virtues of the GA is that it yields an exact result for Coulomb scattering within a constant phase (Wallace 1973). Another virtue of this approximation is that it is approximately unitary. The GA has been applied to both elastic and inelastic collisions of electrons with hydrogen and helium (Franco 1968, 1970, 1973, Tai *et al* 1969a, b, 1970, Ghosh and Sil 1969, 1970, Bhadra and Ghosh 1971, Yates and Tenny 1972, Thomas and Chan 1973, Chan and Chen 1973, 1974, Chan and Chang 1975, Kamal *et al* 1976) with success. However, the success is greater in the case of inelastic collisions than in elastic processes.

Chutjian and Thomas (1975) have reported measurements of normalised absolute differential and integral scattering cross sections for the electron-impact optically-forbidden transition $^1S(1s, 3s) \leftarrow {}^1S(1s)^2$ in helium at 29·2 and 39·7 eV. They have also examined this transition process within the framework of first-order many-body theory (FOMBT) (Csanak *et al* 1971) and pointed out that FOMBT is not quite successful in predicting the magnitudes of differential cross sections (DCS), but it predicts their shape. Scott and McDowell (1975) have applied the distorted-wave polarised orbital approximation (DWPOA) to compute integral and differential cross sections at impact energies between 30 and 300 eV. At low energies ($E < 100$ eV) they reproduce the shape of the

0022-3700/79/030497+14$01.00

DCS but are unsuccessful in predicting the depth of the minimum. A few other calculations (Baye and Heenen 1974, Winters *et al* 1977, Bransden and Issa 1975, Flannery and McCann 1975) have been performed at incident energies greater than 50 eV. In this energy range experimental data for integral cross sections are available, but unfortunately there are no measurements of DCS. The GA has been applied to the excitation of the 2^1S state of He by electron impact by a number of authors (Yates and Tenny 1972, Franco 1973, Chan and Chen 1973) with considerable success, but to the best of our knowledge, it has not been applied to the case of 3^1S excitation of helium.

This paper reports an application of the GA to the electron-impact transition $^1S(1s, 3s) \leftarrow {}^1S(1s)^2$ in helium in the energy range 29·2 to 500 eV. The principal objective is to see how far the GA is successful in predicting cross sections for the above-mentioned process. We shall concentrate, in particular, upon electron energies of 30 to 50 eV where a large number of inelastic channels open up and where absolute differential and integral cross sections are available. In this energy region close-coupling calculations do not seem to be feasible and simple first-order theories, such as those following Born and Ochkur, are reported to have been unsuccessful (Chutjian and Thomas 1975).

Section 2 presents the GA theory as applied to the excitation of atomic helium from its ground state to the 3^1S state. In that section we have given an account of our formulation for evaluating the modified Lommel function in integral form. Section 3 contains an analysis of results. Conclusions are given in § 4. Unless otherwise stated, atomic units are used throughout the paper.

2. Theory

The Glauber amplitude $F_{fi}(\boldsymbol{q})$ for the scattering of an electron from atomic helium is given by (Thomas and Chan 1973)

$$F_{fi}(\boldsymbol{q}) = \frac{ik}{2\pi} \int d\boldsymbol{b}\, d\boldsymbol{r}_1\, d\boldsymbol{r}_2 \phi_f^*(\boldsymbol{r}_1, \boldsymbol{r}_2) \Gamma(\boldsymbol{b}; \boldsymbol{r}_1, \boldsymbol{r}_2) \phi_i(\boldsymbol{r}_1, \boldsymbol{r}_2)\, e^{i\boldsymbol{q}.\boldsymbol{b}} \tag{1}$$

where

$$\Gamma(\boldsymbol{b}; \boldsymbol{r}_1, \boldsymbol{r}_2) = 1 - \left(\frac{|\boldsymbol{b} - \boldsymbol{s}_1|}{b}\right)^{2i\eta} \left(\frac{|\boldsymbol{b} - \boldsymbol{s}_2|}{b}\right)^{2i\eta} \tag{2}$$

and

$$\eta = 1/k.$$

Here k is the wavenumber of the incident particle; $\boldsymbol{b}$, $\boldsymbol{s}_1$, $\boldsymbol{s}_2$ denote the respective projections of the position vectors of the projectile and the bound electrons $\boldsymbol{r}_1$ and $\boldsymbol{r}_2$ onto the plane perpendicular to the direction of the Glauber path integration; $\boldsymbol{q}$ stands for the momentum transfer vector which lies in the plane of $\boldsymbol{b}$; ϕ_i and ϕ_f are respectively the normalised initial and final atomic wavefunctions which are orthogonal to each other. In the present case the initial state is the ground state $^1S(1s)^2$ whereas the final state is $^1S(1s, 3s)$.

The helium wavefunctions ϕ_i and ϕ_f we have chosen are such that the product $\phi_f^* \phi_i$ may be expressed as

$$\phi_f^* \phi_i = (4\pi)^{-2} \sum_{i=1}^{N} p_i\, e^{-\mu_i r_1} r_1^{\rho_i}\, e^{-\nu_i r_2} r_2^{\delta_i}. \tag{3}$$

Equation (3) can be written as

$$\phi_f^* \phi_i = (4\pi)^{-2} \sum_{i=1}^{N} p_i (-1)^{1+\rho_i} \left(\frac{\partial}{\partial \mu_i}\right)^{1+\rho_i} \frac{e^{-\mu_i r_1}}{r_1} (-1)^{1+\delta_i} \left(\frac{\partial}{\partial \nu_i}\right)^{1+\delta_i} \frac{e^{-\nu_i r_2}}{r_2}. \tag{4}$$

Substituting equation (4) into equation (1), we have

$$F_{fi}(\boldsymbol{q}) = \frac{ik}{32} \sum_{i=1}^{N} p_i (-1)^{\rho_i+\delta_i} \left(\frac{\partial}{\partial \mu_i}\right)^{1+\rho_i} \left(\frac{\partial}{\partial \nu_i}\right)^{1+\delta_i} I(\mu_i, \nu_i, q) \tag{5}$$

where we define

$$I(\mu, \nu, q) = \frac{1}{\pi^3} \int d\boldsymbol{b}\, d\boldsymbol{r}_1\, d\boldsymbol{r}_2\, e^{i\boldsymbol{q}.\boldsymbol{b}} \frac{1}{r_1 r_2} e^{-\mu r_1 - \nu r_2} \left[1 - \left(\frac{|\boldsymbol{b}-\boldsymbol{s}_1|}{b}\right)^{2i\eta} \left(\frac{|\boldsymbol{b}-\boldsymbol{s}_2|}{b}\right)^{2i\eta}\right]. \tag{6}$$

We break up the full Γ of equation (2) in a fashion analogous to the Glauber multiple-scattering expansion (Glauber 1959):

$$\Gamma(\boldsymbol{b}; \boldsymbol{r}_1, \boldsymbol{r}_2) = \Gamma_1(\boldsymbol{b}; \boldsymbol{r}_1) + \Gamma_2(\boldsymbol{b}; \boldsymbol{r}_2) - \Gamma_1(\boldsymbol{b}; \boldsymbol{r}_1)\Gamma_2(\boldsymbol{b}; \boldsymbol{r}_2) \tag{7}$$

where

$$\Gamma_i(\boldsymbol{b}; \boldsymbol{r}_i) = 1 - \left(\frac{|\boldsymbol{b}-\boldsymbol{s}_i|}{b}\right)^{2i\eta}.$$

Here the sum $\Gamma_1 + \Gamma_2$ contains the effects of single-particle scattering from each of the charged particles comprising the helium atom, together with higher-order scattering.

Next we introduce spherical polar coordinates for $\boldsymbol{r}_1$ and $\boldsymbol{r}_2$, and obtain

$$\begin{aligned} I(\mu, \nu, q) = {} & \frac{(4\pi)^{1/2}}{\pi^3} \int d\boldsymbol{b}\, e^{i\boldsymbol{q}.\boldsymbol{b}} \int dr_1\, r_1\, e^{-\mu r_1} \int dr_2\, r_2\, e^{-\nu r_2} \int d\hat{\boldsymbol{r}}_2 \int d\hat{\boldsymbol{r}}_1\, Y_{00}(\hat{\boldsymbol{r}}_1) \\ & \times \left[1 - \left(\frac{|\boldsymbol{b}-\boldsymbol{s}_1|}{b}\right)^{2i\eta}\right] + \frac{(4\pi)^{1/2}}{\pi^3} \int d\boldsymbol{b}\, e^{i\boldsymbol{q}.\boldsymbol{b}} \int dr_2\, r_2\, e^{-\nu r_2} \\ & \times \int dr_1\, r_1\, e^{-\mu r_1} \int d\hat{\boldsymbol{r}}_1 \int d\hat{\boldsymbol{r}}_2\, Y_{00}(\hat{\boldsymbol{r}}_2) \left[1 - \left(\frac{|\boldsymbol{b}-\boldsymbol{s}_2|}{b}\right)^{2i\eta}\right] \\ & - \frac{4}{\pi^2} \int d\boldsymbol{b}\, e^{i\boldsymbol{q}.\boldsymbol{b}} \int dr_1\, r_1\, e^{-\mu r_1} \int d\hat{\boldsymbol{r}}_1\, Y_{00}(\hat{\boldsymbol{r}}_1) \left[1 - \left(\frac{|\boldsymbol{b}-\boldsymbol{s}_1|}{b}\right)^{2i\eta}\right] \\ & \times \int dr_2\, r_2\, e^{-\nu r_2} \int d\hat{\boldsymbol{r}}_2\, Y_{00}(\hat{\boldsymbol{r}}_2) \left[1 - \left(\frac{|\boldsymbol{b}-\boldsymbol{s}_2|}{b}\right)^{2i\eta}\right]. \end{aligned} \tag{8}$$

Utilising the result of Thomas and Franco (1976) that

$$\begin{aligned} & \frac{1}{2\pi} \int d\hat{\boldsymbol{r}}\, Y_{lm}^*(\hat{\boldsymbol{r}}) \left[1 - \left(\frac{|\boldsymbol{b}-\boldsymbol{s}|}{b}\right)^{2i\eta}\right] \\ & = 2(-1)^{(l-m)/2} Y_{lm}^*(\pi/2, \phi_b) \left\{ \delta_{l,0}\delta_{m,0} + 2^{2i\eta} \frac{\Gamma(1+i\eta)}{\Gamma(1-i\eta)} \right. \\ & \left. \times \int_0^\infty dt\, t^{-2i\eta} \frac{d}{dt} \left[J_m(t) \left(\frac{\pi b}{2rt}\right)^{1/2} J_{l+\frac{1}{2}}\left(\frac{rt}{b}\right) \right] \right\} \end{aligned}$$

and performing the radial integrations over r_1 and r_2 we get

$$I(\mu, \nu, q) = 32(\mu\nu)^{-2} \int_0^\infty b \, \mathrm{d}b \, J_0(qb) - 32 \, g^2(\eta) \int_0^\infty b^5 \, \mathrm{d}b \, J_0(qb)$$
$$\times \int_0^\infty \mathrm{d}t_1 t_1^{-2i\eta} \frac{\mathrm{d}}{\mathrm{d}t_1}\left(\frac{J_0(t_1)}{t_1^2+\mu^2 b^2}\right) \int_0^\infty \mathrm{d}t_2 \, t_2^{-2i\eta} \frac{\mathrm{d}}{\mathrm{d}t_2}\left(\frac{J_0(t_2)}{t_2^2+\nu^2 b^2}\right) \tag{9}$$

where

$$g(\eta) = 2^{2i\eta} \frac{\Gamma(1+i\eta)}{\Gamma(1-i\eta)}.$$

Equation (9) has been obtained earlier (Thomas and Chan 1973) using cylindrical coordinates for $\boldsymbol{r}_1$ and $\boldsymbol{r}_2$.

Next we adopt their procedure to remove explicitly the two-dimensional delta function $\delta(\boldsymbol{q})$ stemming from the first term in equations (6) and (9). The result is

$$I(\mu, \nu, q) = -2^4(2i\eta)^2\Gamma(i\eta)\Gamma(1-i\eta)q^{-4}[\nu^{-2}H(\mu q^{-1}, \eta) + \mu^{-2}H(\nu q^{-1}, \eta)]$$
$$-2^5(2i\eta)^2 g^2(\eta) \int_0^\infty b^5 \, \mathrm{d}b \, J_0(qb) K(\mu b, \eta) K(\nu b, \eta) \tag{10}$$

where

$$H(x, \eta) = x^{-2i\eta-2} {}_2F_1(1-i\eta, 1-i\eta; 1; -x^2) \tag{11}$$

and

$$K(x, \eta) = \frac{1}{x^2} \int_0^\infty \mathrm{d}t \, t^{-2i\eta+1} \frac{J_0(t)}{t^2+x^2}. \tag{12}$$

Equation (10) is essentially the same as equation (19) of Thomas and Chan (1973) except that the modified Lommel function will now be computed via a representation involving an infinite integral. In the following we describe a method for the efficient evaluation of the K integral. This method can be conveniently used to obtain convergent results for the modified Lommel function for intermediate values of the argument where the series representation requires extremely high precision.

To do the K integral we break it up into two parts:

$$K = K_{1,n} + K_{2,n} \tag{13}$$

where

$$x^2 K_{1,n} = \int_0^{t_0} \mathrm{d}t \, t^{-2i\eta+1} \frac{J_0(t)}{(t^2+x^2)^n} \tag{14}$$

and

$$x^2 K_{2,n} = \int_{t_0}^\infty \mathrm{d}t \, t^{-2i\eta+1} \frac{J_0(t)}{(t^2+x^2)^n}. \tag{15}$$

Utilising the approximation for $J_0(t)$ in the range $-3 \leqslant t \leqslant 3$ (Abramowitz and Stegun 1965, p 369) the $K_{1,n}$ integral can be expressed as

$$K_{1,n} \equiv \int_0^{t_0} \mathrm{d}t \, t^{-2i\eta+1} \frac{1}{(t^2+x^2)^n}\left(1 + \sum_{\alpha=1}^{6} g_\alpha t'^{2\alpha}\right)$$

with $t' = t/3$.

Now writing $t = t_0 \, e^{-\frac{1}{2}y}$ we get

$$K_{1,n} = \tfrac{1}{2} t_0^{-2i\eta+2} \int_0^\infty dy \, e^{-y} \frac{[\cos(\eta y) + i \sin(\eta y)]}{(t_0^2 \, e^{-y} + x^2)^n} \left(1 + \sum_{\alpha=1}^{6} g_\alpha \, e^{-y\alpha}\right). \tag{16}$$

For the evaluation of $K_{2,n}$, we again use the approximate expression for J_0 in the energy range $3 \leqslant t < \infty$ (Abramowitz and Stegun 1965, p 369). Equation (15) then becomes

$$K_{2,n} \equiv \int_{t_0}^\infty dt \, t^{-2i\eta+1} \frac{1}{(t^2+x^2)^n} \left[t^{-1/2} \left(c_1 + \sum_{\alpha=1}^{6} a_\alpha t'^\alpha \right) \cos\left(c_2 + t + \sum_{\alpha=1}^{6} b_\alpha t'^\alpha \right) \right] \tag{17}$$

with $t' = t_0/t$.

Equation (17) can be expressed as

$$K_{2,n} = \int_{t_0}^\infty (e^{i(t+c_2+\phi(t))} + e^{-i(t+c_2+\phi(t))}) F(t) \, dt \tag{18}$$

where

$$\phi(t) = \sum_{\alpha=1}^{6} b_\alpha t'^\alpha$$

and

$$F(t) = \tfrac{1}{2} t^{-2i\eta+\frac{1}{2}} \frac{1}{(t^2+x^2)^n} \left(c_1 + \sum_{\alpha=1}^{6} a_\alpha t'^\alpha \right).$$

We consider the first integral along the path t_0 to ∞ on the real axis. Instead of taking this contour we rotate it around t_0 in the counter-clockwise direction so that the new path becomes vertical along t_0 to $t_0 + i\infty$. We note that while rotating, no singularity is crossed and that the integrand vanishes at infinity. Hence by Cauchy's theorem the integral along the new path is the same as the integral along the previous path. Similarly, the second integral can be transformed to a new equivalent integral along the path t_0 to $t_0 - i\infty$ by rotating the contour in the clockwise direction.

Substituting $t = t_0 + iy$ in the first integral and $t = t_0 - iy$ in the second integral we can write

$$K_{2,n} = \int_0^\infty dy \, e^{-y} \{ [R(A+iB)(C+iD) \exp(E+iF)] + [R'(A'+iB')(C'+iD') \exp(E'+iF')] \} \tag{19}$$

where

$$A = -\tfrac{1}{2} \sin(c_2 + t_0) = A' \qquad B = \tfrac{1}{2} \cos(c_2 + t_0) = -B'$$

$$R = \rho^{1/2} \, e^{2\eta\phi} \rho'^{-n} \qquad \rho = (t_0^2 + y^2)^{1/2} \qquad \phi = \tan^{-1}(y/t_0)$$

$$C = c_1 + \sum_{\alpha=1}^{6} a_\alpha t_0^\alpha \rho^{-\alpha} \cos(\phi\alpha) \qquad D = -\sum_{\alpha=1}^{6} a_\alpha t_0^\alpha \rho^{-\alpha} \sin(\phi\alpha)$$

$$E = \sum_{\alpha=1}^{6} b_\alpha t_0^\alpha \rho^{-\alpha} \sin(\phi\alpha) \qquad F = \sum_{\alpha=1}^{6} b_\alpha t_0^\alpha \rho^{-\alpha} \cos(\phi\alpha) + (-n\phi' + \phi/2 - 2\eta \ln \rho)$$

$$\rho' = \{ [\rho^2 \cos(2\phi) + x^2]^2 + [\rho^2 \sin(2\phi)]^2 \}^{1/2}$$

$$\phi' = \tan^{-1}\{ [\rho^2 \sin(2\phi)] / [\rho^2 \cos(2\phi) + x^2] \}$$

$$R' = \rho^{1/2} e^{2\eta\bar{\phi}} \bar{\rho}'^{-n} \qquad \bar{\rho}' = \{[\rho^2 \cos(2\bar{\phi}) + x^2]^2 + [\rho^2 \sin(2\bar{\phi})]^2\}^{1/2}$$

$$\bar{\phi} = \tan^{-1}(-y/t_0) \qquad \bar{\phi}' = \tan^{-1}\{[\rho^2 \sin(2\bar{\phi})]/[\rho^2 \cos(2\bar{\phi}) + x^2]\}$$

$$C' = c_1 + \sum_{\alpha=1}^{6} a_\alpha t_0^\alpha \rho^{-\alpha} \cos(\bar{\phi}\alpha) \qquad D' = -\sum_{\alpha=1}^{6} a_\alpha t_0^\alpha \rho^{-\alpha} \sin(\bar{\phi}\alpha)$$

$$E' = -\sum_{\alpha=1}^{6} b_\alpha t_0^\alpha \rho^{-\alpha} \sin(\bar{\phi}\alpha) \qquad F' = -\sum_{\alpha=1}^{6} b_\alpha t_0^\alpha \rho^{-\alpha} \cos(\bar{\phi}\alpha) + (-n\bar{\phi}' + \tfrac{1}{2}\bar{\phi} - 2\eta \ln \rho).$$

The integrals $K_{1,n}$ and $K_{2,n}$ given by equations (16) and (19) can now be evaluated by numerical integration using Gauss–Laguerre quadratures (Abramowitz and Stegun 1965, p 923). The purpose of obtaining equations (16) and (19) is to obtain forms which do not exhibit rapid oscillations over the region of integration, so that standard numerical integration procedures will converge rapidly. However, for very small values of x, the following closed form expression (Watson 1966) has been used for the evaluation of the K integral.

$$\int_0^\infty t^{-2i\eta-1+2\omega+M_j}(t^2+\gamma^2)^{-1-M_j-2p} J_{M_j}(t)\,dt$$
$$= 2^{-1-M_j}\gamma^{-2i\eta+2\omega-4p-2} E_1(\eta)\, {}_1F_2(M_j+\omega-i\eta;\ \omega-2p-i\eta,\ M_j+1;\ \tfrac{1}{4}\gamma^2)$$
$$+ 2^{-M_j-4p-3+2\omega-2i\eta} E_2(\eta)$$
$$\times {}_1F_2(M_j+2p+1;\ 2+M_j+2p-\omega+i\eta,\ 2p+2-\omega+i\eta;\ \tfrac{1}{4}\gamma^2) \qquad (20)$$

where

$$E_1(\eta) = \Gamma(M_j+\omega-i\eta)\Gamma(2p+1-\omega+i\eta)[(M_j+2p)!M_j!]^{-1}$$

and

$$E_2(\eta) = \Gamma(\omega-2p-1-i\eta)/\Gamma(2+M_j+2p-\omega+i\eta).$$

The scattering amplitude is obtained by substituting equation (10) into equation (5) and differentiating:

$$F_{fi}(\boldsymbol{q}) = A_1 \sum_{i=1}^{N} p_i(-1)^{\rho_i+\delta_i}\Big((-1)^{1+\delta_i}\frac{(2+\delta_i)!}{(\nu_i)^{3+\delta_i}} H(\mu q^{-1},\ \eta,\ 1+\rho_i)$$
$$+ (-1)^{1+\rho_i}\frac{(2+\rho_i)!}{(\mu_i)^{3+\rho_i}} H(\nu q^{-1},\ \eta,\ 1+\delta_i)\Big)$$
$$+ A_2 \int_0^\infty b^5\, db J_0(qb) \sum_{i=1}^{N} p_i(-1)^{\rho_i+\delta_i} K(\mu b,\ \eta,\ 1+\rho_i) K(\nu b,\ \eta,\ 1+\delta_i) \qquad (21)$$

where

$$A_1 = 2ik\eta^2\Gamma(i\eta)\Gamma(1-i\eta)q^{-4} \qquad A_2 = 4ik\eta^2 g^2(\eta)$$

$$H(\mu q^{-1},\ \eta,\ n) = \left(\frac{\partial}{\partial\mu}\right)^n H(\mu q^{-1},\ \eta) \qquad K(\nu b,\ \eta,\ n) = \left(\frac{\partial}{\partial\nu}\right)^n K(\nu b,\ \eta).$$

The H functions for different values of n are obtained via (Magnus *et al* 1966)

$$\frac{d}{dx}\, {}_2F_1(a, b; c; x) = abc^{-1}\, {}_2F_1(a+1, b+1; c+1; x)$$

whereas the K functions are evaluated by analytic differentiation and by using equations (16), (19) and (20).

An approximation to the GA, called the single-particle Glauber approximation (SPGA) is obtained by taking into consideration only the effects of single-particle scattering in the Glauber formalism; this however means ignoring the third term of the profile function $\Gamma(\boldsymbol{b}; \boldsymbol{r}_1, \boldsymbol{r}_2)$ given by equation (7). It can be shown that this approximate form of the profile function yields the terms in equation (21) which involve the hypergeometric functions. At high energies and small scattering angles where single-particle scattering is predominant, the SPGA seems to be a reasonable approximation.

3. Numerical results and discussion

We have computed both the differential and integral cross sections for the electron-impact excitation of the 3^1S state of He in the first Born approximation (FBA), the SPGA and the GA in the energy range 29·2 to 500 eV. In all these calculations we have used an orthonormal set of wavefunctions. The ground state of He is represented by the approximate Hartree–Fock wavefunction of Green *et al* (1954):

$$\phi(1^1S|\boldsymbol{r}_1, \boldsymbol{r}_2) = u(r_1)u(r_2)$$

where

$$u(r) = 0{\cdot}8373888\ (e^{-\beta r} + 0{\cdot}6\ e^{-2\beta r})$$

$$\beta = 1{\cdot}455799.$$

The wavefunction of the $^1S(1s, 3s)$ state of He is of the Eckart form as determined by Winter and Lin (1975):

$$\phi(3^1S|\boldsymbol{r}_1, \boldsymbol{r}_2) = 2^{-1/2}N\{\psi(3^1S|\boldsymbol{r}_1)\psi_0[z(3^1S)|r_2] + \psi_0[z(3^1S)|r_1]\psi(3^1S|\boldsymbol{r}_2)\}$$

where

$$\psi(3^1S|\boldsymbol{r}) = (4\pi)^{-1/2}\ e^{-ar}(b_1 - b_2 r + b_3 r^2)$$

$$\psi_0[z(3^1S)|r] = (z^3/\pi)^{1/2}\ e^{-zr}$$

$a = 0{\cdot}360$, $b_1 = 0{\cdot}2998203$, $b_2 = 0{\cdot}2631616$, $b_3 = 0{\cdot}03434894$, $N = 0{\cdot}9994284$ and $z = 2{\cdot}0$.

The wavefunction ϕ and one-electron function ψ are normalised individually and $\phi(n^1S|\boldsymbol{r}_1, \boldsymbol{r}_2)$ is made orthogonal to each $\phi(n'^1S|\boldsymbol{r}_1, \boldsymbol{r}_2)$ for $n' < n$. Although the present set of wavefunctions is very simple it yields FBA cross sections in reasonable agreement with the corresponding results obtained with the extremely elaborate correlated wavefunctions of Bell *et al* (1969).

The SPGA amplitude is obtained from an efficient program for calculating the hypergeometric functions. These functions occurring in the H functions of equation (20) were calculated first by applying the linear transformation (Magnus *et al* 1966):

$${}_2F_1(a, b; c; z) = (1-z)^{-a}\ {}_2F_1(a, c-b; c; z/(z-1))$$

and then summing the resultant hypergeometric series. For large values of z however,

we have adopted the following form (Abramowitz and Stegun 1965, p 560):

$$
\begin{aligned}
&{}_2F_1(a, a; c; z) \\
&\quad = \frac{\Gamma(c)}{\Gamma(a)\Gamma(c-a)}(-z)^{-a} \sum_{n=0}^{\infty} \frac{(a)_n(1-c+a)_n}{(n!)^2} z^{-n}[\ln(-z) + 2\psi(n+1) \\
&\qquad - \psi(a+n) - \psi(c-a-n)]
\end{aligned}
$$

($|\arg(-z)| < \pi$; $|z| > 1$; $(c-a) \neq 0, \pm 1, \pm 2, \ldots$).

The Glauber amplitude is evaluated by dividing the infinite integral over b into a number of intervals: sufficient intervals are taken so as to obtain convergence. In order to check the accuracy of our program we have computed the K function for small values of x from equation (20) as well as from the present technique utilising (16) and (19). For different values of η and n we have found that the two procedures agree up to five significant figures. For a simultaneous check on the integration routine and the numerical evaluation of the K functions, we have verified equation (18) of Thomas and Chan (1973) to a high degree of accuracy. Moreover, we have calculated the e^-–He elastic differential cross sections using Hylleraas wavefunctions and found good agreement with the corresponding results of Thomas and Chan (1973) and of Kamal *et al* (1976). This demonstrates that the present procedure is valid and useful for performing practical calculations. In addition, we have calculated the e^+–He scattering cross sections and found that these cross sections are identical with the corresponding e^-–He results. Also we notice from the computed amplitudes that

$$F(\boldsymbol{q})|_{e^+\text{–He}} = -F^*(\boldsymbol{q})|_{e^-\text{–He}}.$$

3.1. Differential cross sections

The DCS calculated in the FBA, the SPGA and the GA for incident electron energies 29·2 and 39·7 eV are listed in tables 1 and 2 respectively, together with the experimental data of Chutjian and Thomas (1975). Additional DCS results obtained in the SPGA and the GA for electron energies 80, 100, 200 and 500 eV are given in table 3. The reported results are for the experimental energies of the initial and final states of He. We see that the FBA and the SPGA are unable to predict the observed structures in the experimental DCS at 29·2 and 39·7 eV. The GA, on the other hand, is capable of predicting the angular distributions. At 500 eV (table 3) we notice that the SPGA and the GA yield cross sections close to each other. However, the agreement decreases as the scattering angle increases. With a decrease in energy the SPGA deviates strongly from the GA. While at 500 eV the cross section value of the SPGA differs from that of the GA by nearly 2% in the forward direction, this difference is about 115% at 29·2 eV.

For comparison, in figures 1 to 4 we have displayed our DCS results calculated in the FBA, the SPGA and the GA in addition to the results of other theoretical calculations and of experiments. The shapes and trends of the present calculations are similar to those obtained by theoretical studies of the 2^1S excitation (Yates and Tenny 1972, Franco 1973, Chan and Chen 1973).

Figure 1 is concerned with scattering at 29·2 eV. At this energy the experiment of Chutjian and Thomas (1975) shows a minimum at 45°, a plateau between 60° and 90° and a rise thereafter. We see that both the FBA and the SPGA fail to produce the observed structure of the DCS. The calculated GA curve lies below experiment at angles less than 40° and has a minimum which is quite deep. The magnitudes of the GA cross

Table 1. Differential cross sections in units of 10^{-20} cm^2 sr^{-1} for the 3^1S excitation of helium by 29·2 eV electrons.

Angle (deg)	FBA	SPGA	GA	Experiment
0	20·9	8·8	4·1	—
5	20·8	8·6	3·9	41
10	20·2	8·1	3·6	27
20	18·3	6·3	2·5	9·9
30	15·6	4·3	1·5	2·4
35	14·1	3·4	1·0	1·6
40	12·6	2·7	0·69	0·34
45	11·1	2·1	0·44	0·24
50	9·67	1·6	0·27	0·26
55	8·38	1·2	0·16	0·57
60	7·21	0·94	0·10	0·61
68	5·61	0·63	0·068	0·71
75	4·47	0·47	0·079	0·65
90	2·75	0·31	0·14	0·83
100	2·02	0·27	0·19	1·2
105	1·74	0·26	0·21	1·6
112	1·42	0·26	0·23	2·3
120	1·15	0·26	0·25	3·8
128	0·951	0·26	0·27	4·4
136	0·803	0·26	0·28	4·9

Table 2. Differential cross sections in units of 10^{-20} cm^2 sr^{-1} for the 3^1S excitation of helium by 39·7 eV electrons.

Angle (deg)	FBA	SPGA	GA	Experiment
0	39	33	22	—
5	39	32	21	91
10	37	28	17	53
15	34	22	13	26
20	30	17	10	11
25	26	13	6·5	3·2
30	22	9·0	4·2	0·83
45	12	3·0	0·85	0·46
60	5·4	1·0	0·23	0·18
75	2·3	0·53	0·28	0·20
90	1·0	0·41	0·38	1·1
105	0·48	0·37	0·43	2·3
110	0·38	0·37	0·43	2·3
120	0·24	0·36	0·43	2·7
136	0·13	0·34	0·42	5·9

sections differ substantially from the measured values particularly at small angles. In the present work the GA minimum lies near 68° with a minimum cross section of 7×10^{-22} cm^2 sr^{-1}, whereas the experimental minimum lies near 45° with a minimum cross section of $2{\cdot}4\times10^{-21}$ cm^2 sr^{-1}which is about three times as large as the GA value. The results of the FOMBT which are displayed in figure 1 lie below those of experiment at angles less than 30° and have a very deep minimum at about 60° which is smaller than the measured minimum by a factor of about 60.

Table 3. Differential cross sections in units of 10^{-20} cm^2 sr^{-1} for the 3^1S excitation of helium by electron impact.

Angle (deg)	SPGA 80 eV	GA 80 eV	SPGA 100 eV	GA 100 eV	SPGA 200 eV	GA 200 eV	SPGA 500 eV	GA 500 eV
0	97	82	111	98	131	125	129	127
2	94	80	107	94	120	113	104	101
4	87	73	98	84	101	93	78	75
6	78	65	84	72	78	71	58	54
8	68	55	71	59	62	56	39	37
10	58	46	59	48	49	43	25	23
12	49	38	49	39	37	32	15	14
14	41	31	40	31	28	23	8·7	7·7
16	34	25	33	25	21	17	4·9	4·3
18	28	20	26	19	15	12	2·7	2·3
20	23	16	21	15	11	8·2	1·5	1·3
25	14	8·7	12	7·6	4·3	3·2	0·37	0·44
30	8·1	4·5	6·4	3·7	1·8	1·3	0·13	0·25
35	4·7	2·3	3·4	1·8	0·79	0·74	0·66(−1)	0·17
40	2·7	1·2	1·9	1·0	0·42	0·54	0·42(−1)	0·13
45	1·6	0·79	1·1	0·73	0·26	0·45	0·30(−1)	0·96(−1)
50	1·0	0·62	0·72	0·63	0·19	0·39	0·22(−1)	0·73(−1)
55	0·73	0·58	0·52	0·59	0·14	0·33	0·16(−1)	0·56(−1)
60	0·56	0·57	0·41	0·57	0·12	0·29	0·13(−1)	0·43(−1)
68	0·42	0·57	0·31	0·53	0·85(−1)	0·22	0·85(−2)	0·30(−1)
75	0·36	0·55	0·26	0·48	0·66(−1)	0·18	0·63(−2)	0·22(−1)
90	0·27	0·47	0·19	0·37	0·41(−1)	0·12	0·36(−2)	0·13(−1)
100	0·23	0·41	0·15	0·31	0·31(−1)	0·90(−1)	0·26(−2)	0·94(−2)
105	0·21	0·38	0·14	0·29	0·28(−1)	0·80(−1)	0·23(−2)	0·83(−2)
112	0·19	0·35	0·12	0·26	0·24(−1)	0·70(−1)	0·19(−2)	0·70(−2)
120	0·17	0·32	0·11	0·23	0·20(−1)	0·60(−1)	0·16(−2)	0·59(−2)

Figure 2 displays the present FBA, SPGA and GA cross sections at 39·7 eV along with the results of the FOMBT calculation and the experimental data. Here the experiment shows that the plateau observed at 29·2 eV (figure 1) has almost disappeared and that the minimum has broadened and shifted to a larger scattering angle. As in figure 1, we see that both the FBA and the SPGA fail once again to predict the structure of the DCS. The GA curve at this energy again lies below the experimental curve at small angles, less than 25°, but otherwise has the same general shape. Here the minimum has been found at a scattering angle of 68° while the experimental minimum lies at about 60°. These two minimum values differ in magnitude by not more than 25% whereas the corresponding results at 29·2 eV differed by a factor of 3. In this case the FOMBT curve lies below experiment at angles less than 20° and shows a minimum at an angle of 60° but its magnitude differs from that of experiment by a factor of about 2·5. With an increase in energy we see that the magnitudes of the GA cross sections are closer to those of the experimental cross sections. The improvement is substantial. In the forward direction where the discrepancy between the GA and experiment is greatest we note that whereas the GA cross section at 29·2 eV differs from the experimental result by a factor of 12, this factor is about 3 at 39·7 eV. Nevertheless the discrepancy between the GA and experiment is still large. Such is also the case with the FOMBT. The DWPOA has also failed to predict the magnitudes of cross sections at small

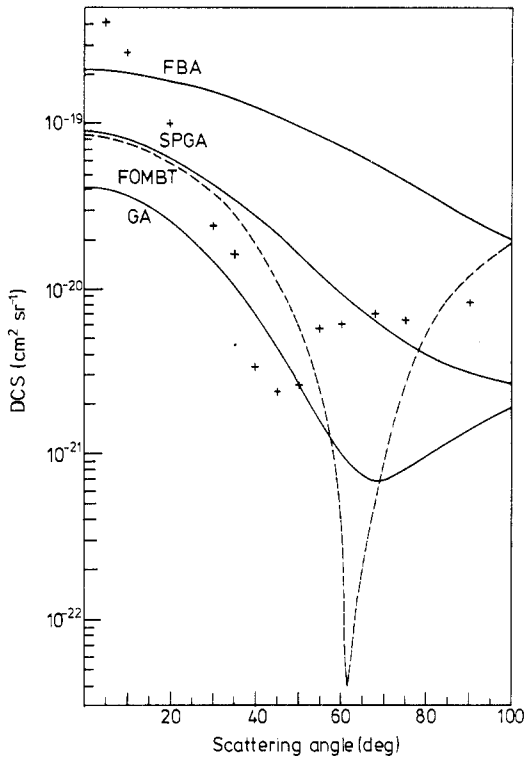

Figure 1. Differential cross sections for the excitation of the ^{1}S(1s,3s) state of He by electron impact at 29·2 eV. FBA, the present first Born approximation; SPGA, the present single-particle Glauber approximation; GA, the present full Glauber approximation; FOMBT, the first-order many-body theory (Chutjian and Thomas 1975); +, experimental results of Chutjian and Thomas.

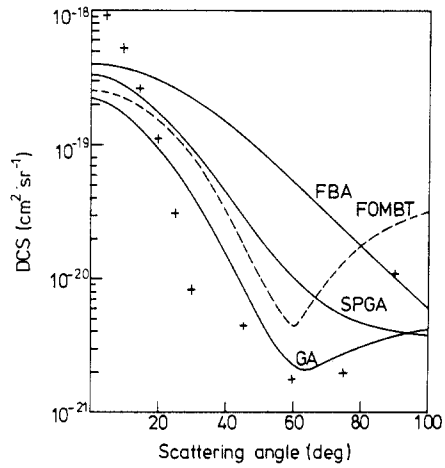

Figure 2. Differential cross sections for the excitation of the ^{1}S(1s,3s) state of He by electron impact at 39·7 eV. FBA, the present first Born approximation; SPGA, the present single-particle Glauber approximation; GA, the present full Glauber approximation; FOMBT, the first-order many-body theory (Chutjian and Thomas 1975); +, experimental results of Chutjian and Thomas.

angles at energies of 29·2 and 39·7 eV. This method has reproduced the shape of the experimental DCS but has been unable to predict the depth of the minimum.

Figures 3 and 4 show the present FBA, SPGA and GA cross sections at energies of 100 and 500 eV respectively, in addition to the results of the second-order optical-potential approximation (SOOPA) which includes nine eigenstates of He. It is seen that the GA curves lie close to the SOOPA curves. At 500 eV the SPGA and the GA nearly coincide in the forward direction, but they begin to diverge with an increase in scattering angle. With a decrease in energy, the discrepancy between these two methods increases. This suggests that the SPGA might be reasonable at low angles and high energies. The shapes and trends of the FBA and the SPGA are similar.

3.2. Integral cross sections

Table 4 presents the integral cross sections calculated in the FBA, the SPGA and the GA along with the corresponding measured values in the energy range 29·2 to 500 eV. At energies greater than 80 eV the GA gives better agreement with the experimental

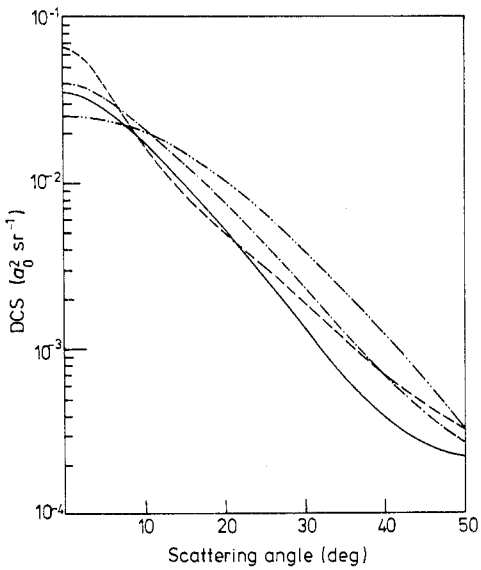

Figure 3. Differential cross sections for the excitation of the ^{1}S(1s,3s) state of He by electron impact at 100 eV. – · · –, the present first Born approximation; – · –, the present single-particle Glauber approximation; ——, the present full Glauber approximation; – –, the second-order optical-potential approximation (Winters *et al* 1977).

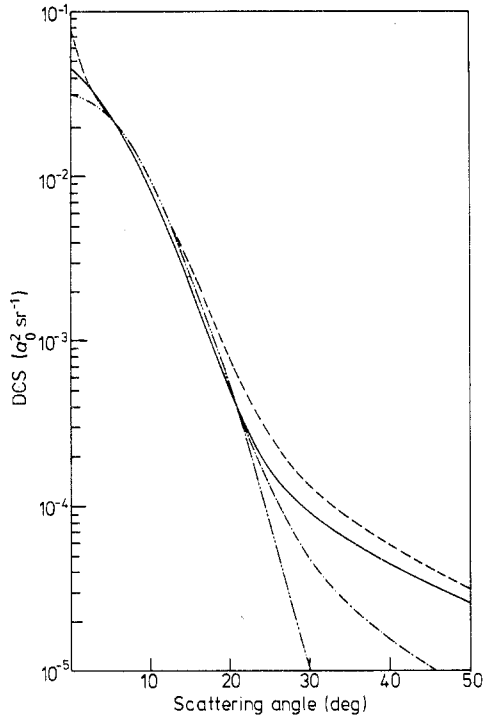

Figure 4. Differential cross sections for the excitation of the ^{1}S(1s,3s) state of He by electron impact at 500 eV. – · · –, the present first Born approximation; – · –, the present single-particle Glauber approximation; ——, the present full Glauber approximation; – – –, the second-order optical-potential approximation (Winters *et al* 1977).

Table 4. Integral cross sections in units of 10^{-20} cm^2 for the 3^1S excitation of helium by electron impact.

Energy(eV)	FBA	SPGA	GA	Experiment
29·2	63	13	5	35
39·7	62	27	15	44
80·0	39	31	24	29
100·0	32	28	23	26
200·0	17	17	16	16
500·0	7·1	7·6	7·3	8·3

results of Moustafa Moussa *et al* (1969) than the FBA. At lower energies the integral cross sections predicted by the GA substantially differ from the measured data of Chutjian and Thomas (1975). At 29·2 and 39·7 eV the FBA appears to yield integral cross sections better than those of the GA although the former is seen to overestimate considerably the magnitude of the DCS (except for very low scattering angles) and fails to give even qualitatively the shape of the angular distribution throughout the angular

range. The better agreement of the FBA with experiment must therefore be fortuitous. The SPGA is seen to give better agreement with experiment than the FBA and seems to be a reasonable approximation to the GA at energies greater than 80 eV. At lower energies it deviates strongly from the GA.

4. Conclusions

We have presented both the differential and integral cross sections calculated in the FBA, the SPGA and the GA for the electron-impact excitation of the 3^1S state of He in the energy range 29·2 to 500 eV. In order to avoid the usual series representation of the modified Lommel function which requires very high precision arithmetic for intermediate values of the argument we have formulated an alternative procedure for the efficient evaluation of this function to compute the Glauber amplitude.

The GA is strikingly successful in predicting the structures of the DCS at 29·2 and 39·7 eV. However, the success of the GA is greater at 39·7 eV than at 29·2 eV. The depths of the two minima obtained in the GA at these two energies are closer to experiment than those obtained in the FOMBT and the DWPOA. Like the FOMBT and the DWPOA, the GA also fails to predict the magnitudes of the DCS at small angles at these energies. At higher energies the GA is in good agreement with experiment. Both the FBA and the SPGA are unable to reproduce the structures of the DCS at low energies. At energies greater than 80 eV the SPGA seems to be a reasonable approximation to the GA.

Acknowledgment

One of the authors (ACR) gratefully acknowledges the partial support of the University Grants Commission through Grant No F 25-1 (7017)/77 (SR.I).

References

Abramowitz M and Stegun I A 1965 *Handbook of Mathematical Functions* (New York: Dover)
Baye D and Heenen P H 1974 *J. Phys. B: Atom. Molec. Phys.* **7** 938–49
Bell K L, Kennedy D J and Kingston A E 1969 *J. Phys. B: Atom. Molec. Phys.* **2** 26–43
Bhadra K and Ghosh A S 1971 *Phys. Rev. Lett.* **26** 737–9
Bransden B H and Issa M R 1975 *J. Phys. B: Atom. Molec. Phys.* **8** 1088–94
Byron F W Jr and Joachain C J 1977 *Phys. Rep.* **34** 233–324
Chan F T and Chang C H 1975 *Phys. Rev.* A **12** 1383–92
Chan F T and Chen S T 1973 *Phys. Rev.* A **8** 2191–4
—— 1974 *Phys. Rev.* A **9** 2393–7
Chutjian A and Thomas L D 1975 *Phys. Rev.* A **11** 1583–95
Csanak Gy, Taylor H S and Yaris R 1971 *Advances in Atomic and Molecular Physics* vol 7 (New York: Academic) pp 287–361
Flannery M R and McCann K J 1975 *J. Phys. B: Atom. Molec. Phys.* **8** 1716–33
Franco V 1968 *Phys. Rev. Lett.* **20** 709–12
—— 1970 *Phys. Rev.* A **1** 1705–8
—— 1973 *Phys. Rev.* A **8** 2927–37
Gerjuoy E and Thomas B K 1974 *Rep. Prog. Phys.* **37** 1345–431
Ghosh A S and Sil N C 1969 *Indian J. Phys.* **43** 490–1
—— 1970 *Indian J. Phys.* **44** 153–61

Glauber R J 1959 *Lectures in Theoretical Physics* vol 1, ed W E Brittin and L G Dunham (New York: Interscience) pp 315–414
Green L C, Mulder M M, Lewis M N and Woll J W Jr 1954 *Phys. Rev.* **93** 757–61
Kamal A N, Richardson J E and Teshima R 1976 *J. Phys. B: Atom. Molec. Phys.* **9** 923–32
Magnus W, Oberhettinger F and Soni R P 1966 *Formulas and Theorems for the Functions of Mathematical Physics* (New York: Springer) p 47
Moustafa Moussa H R, de Heer F J and Schutten J 1969 *Physica* **40** 517–49
Scott T and McDowell M R C 1975 *J. Phys. B: Atom. Molec. Phys.* **8** 1851–65
Tai H, Bassel R H, Gerjuoy E and Franco V 1970 *Phys. Rev.* A **1** 1819–35
Tai H, Teubner P J and Bassel R H 1969a *Phys. Rev. Lett.* **22** 1415
—— 1969b *Phys. Rev. Lett.* **23** 453
Thomas B K and Chan F T 1973 *Phys. Rev.* A **8** 252–62
Thomas B K and Franco V 1976 *Phys. Rev.* A **13** 2004–22
Wallace S J 1973 *Ann. Phys., NY* **78** 190–257
Watson G N 1966 *A Treatise on the Theory of Bessel Functions* (London: Cambridge University Press) p 434
Winter T G and Lin C C 1975 *Phys. Rev.* A **12** 434–43
Winters K H, Issa M and Bransden B H 1977 *Can. J. Phys.* **55** 1074–82
Yates A C and Tenny A 1972 *Phys. Rev.* A **6** 1451–6